Variations in hydrological connectivity of Australian semiarid landscapes indicate abrupt changes in rainfall-use efficiency of vegetation

Mariano Moreno-de las Heras,[1,2] Patricia M. Saco,[1] Garry R. Willgoose,[1] and David J. Tongway[3]

Received 21 August 2011; revised 22 May 2012; accepted 1 June 2012; published 19 July 2012.

[1] Dryland vegetation frequently shows self-organized spatial patterns as mosaic-like structures of sources (bare areas) and sinks (vegetation patches) of water runoff and sediments with variable interconnection. Good examples are banded landscapes displayed by Mulga in semiarid Australia, where the spatial organization of vegetation optimizes the redistribution and use of water (and other scarce resources) at the landscape scale. Disturbances can disrupt the spatial distribution of vegetation causing a substantial loss of water by increasing landscape hydrological connectivity and consequently, affecting ecosystem function (e.g., decreasing the rainfall-use efficiency of the landscape). We analyze (i) connectivity trends obtained from coupled analysis of remotely sensed vegetation patterns and terrain elevations in several Mulga landscapes subjected to different levels of disturbance, and (ii) the rainfall-use efficiency of these landscapes, exploring the relationship between rainfall and remotely sensed Normalized Difference Vegetation Index. Our analyses indicate that small reductions in the fractional cover of vegetation near a particular threshold can cause abrupt changes in ecosystem function, driven by large nonlinear increases in the length of the connected flowpaths. In addition, simulations with simple vegetation-thinning algorithms show that these nonlinear changes are especially sensitive to the type of disturbance, suggesting that the amount of alterations that an ecosystem can absorb and still remain functional largely depends on disturbance type. In fact, selective thinning of the vegetation patches from their edges can cause a higher impact on the landscape hydrological connectivity than spatially random disturbances. These results highlight surface connectivity patterns as practical indicators for monitoring landscape health.

Citation: Moreno-de las Heras, M., P. M. Saco, G. R. Willgoose, and D. J. Tongway (2012), Variations in hydrological connectivity of Australian semiarid landscapes indicate abrupt changes in rainfall-use efficiency of vegetation, *J. Geophys. Res.*, *117*, G03009, doi:10.1029/2011JG001839.

1. Introduction

[2] In arid and semiarid environments (approx. 41% of the Earth's land surface, [*Reynolds et al.*, 2007]), where rainfall is scarce and evapotranspiration is very high, the development of vegetation is fundamentally limited by the availability of soil moisture [*Rodriguez-Iturbe*, 2000]. Vegetation in these landscapes is spatially heterogeneous and generally consists of a mosaic of patches or clusters with high plant biomass interspaced within a bare soil background [*Macfadyen*, 1950; *Valentin et al.*, 1999; *Tongway and Ludwig*, 2001; *Deblauwe et al.*, 2008]. This "patchy" or "patterned" organization can be explained as an adaptive response of the system, built up by spatial mechanisms of resource redistribution, which enhances plant production in hot spots where soil moisture and other scarce resources (e.g., nutrients, soil) become concentrated [*Noy-Meir*, 1973; *Schlesinger et al.*,1990].

[3] Surface redistribution of water runoff and sediments has been highlighted as one of the main mechanisms explaining the functioning and organization of patchy dryland landscapes [*Wainwright et al.*, 2002; *Ludwig et al.*, 2005; *Saco et al.*, 2007; *Franz et al.*, 2012]. These patterns can be characterized as mosaic-like structures of sources and sinks of water and soil resources with variable interconnection [*Puigdefabregas et al.*, 1999; *Mayor et al.*, 2008; *Mueller et al.*, 2008]. The underlying cause is that water infiltration in bare or barely covered soil patches is impeded

[1]School of Engineering, The University of Newcastle, Callaghan, New South Wales, Australia.
[2]Departamento de Ecología, Universidad de Alcalá, Facultad de Ciencias, Alcalá de Henares, Spain.
[3]CSIRO, Ecosystem Sciences, Canberra, Australian Capital Territory, Australia.

Corresponding author: M. Moreno-de las Heras, Departamento de Ecología, Universidad de Alcalá, Facultad de Ciencias, Campus externo de Alcalá, Ctra. Madrid-Barcelona km 33.600, E-28871 Alcalá de Henares (Madrid), Spain. (mariano.moreno@uah.es)

0148-0227/12/2011JG001839

due to water repellence and surface crusting, but is very effective in vegetated patches due to vegetation-soil feedbacks [*Valentin et al.*, 1999; *Urgeghe et al.*, 2010]. As a result, runoff and the associated sediments and nutrients generated on bare soil areas are transferred downslope to the adjacent vegetation patches, which increases the availability of soil moisture and consequently, enhancing plant growth [*Noy-Meir*, 1973]. Good examples of such vegetation patterns are banded landscapes, as those displayed by Mulga (*Acacia aneura* F. Muell) in large areas of semiarid Australia [*Klausmeier*, 1999; *Greene et al.*, 2001; *Moreno-de las Heras et al.*, 2011a]. In these landscapes, vegetation is spatially distributed in stripes or bands aligned along terrain contours. In banded landscapes, where vegetated patches are arranged perpendicular to the direction of overland flow, redistribution of surface runoff is mostly limited to the local source-sink scale [*Dunkerley and Brown*, 1999; *McDonald et al.*, 2009; *Dunkerley*, 2010]. In other words, the hydrological connectivity of these systems (i.e., the length of connected pathways of water runoff and sediments within the landscape) is low, inhibiting the occurrence of integrated runoff at the hillslope scale for most rainfall events. Indeed, the bands of vegetation are especially effective at obstructing and capturing water runoff, and therefore, they locally increase the availability of soil moisture for plant growth [*Wakelin-King*, 1999; *Tongway and Ludwig*, 2001].

[4] Field observations have shown that in these patterned dryland landscapes there is a close relationship between the hydrological connectivity and ecosystem functionality (i.e., the integrity of ecosystem processes, such as nutrient cycling, water budgeting, primary production) [*Tongway and Ludwig*, 2011]. Disturbances (e.g., wildfires, grazing, firewood and timber harvesting) as well as variations in climate can disrupt the spatial distribution of vegetation, increasing the landscape hydrological connectivity and promoting the loss of water resources from the system and, as a result, affect plant performance and growth [*Wilcox et al.*, 2003; *Wu et al.*, 2000]. The amount of landscape-scale biomass production for given amounts of rainfall (i.e., rainfall-use efficiency) provides a quick and expeditious evaluation tool for assessing the degree of degradation or loss of ecosystem function in these systems [*Le Houerou*, 1984; *Holm et al.*, 2003a]. Landscape simulations by *Ludwig et al.* [1999] indicated that the loss of patchiness in banded Mulga landscapes might cause up to 40% reduction in the rainfall-use efficiency of these ecosystems. In fact, the spatial redistribution of water runoff and sediments is controlled by the spatial organization of vegetation while, at the same time, the maintenance of vegetation in these patchy landscapes is highly dependent on the favorable redistribution of water [*D'Odorico et al.*, 2007; *Saco et al.*, 2007].

[5] Modeling studies have suggested that landscape degradation processes in arid and semiarid ecosystems can take place in an abrupt, rather than gradual manner [*Noy-Meir*, 1975; *Rietkerk et al.*, 2004; *D'Odorico et al.*, 2007]. Therefore, largely irreversible catastrophic shifts from patterned to alternative barren or unproductive ecosystem states (i.e., landscape desertification) may occur in response to external stresses [*May*, 1977; *Walker et al.*, 1981; *Scheffer et al.*, 2001]. Following a similar rationale, *Davenport et al.* [1998] argued that small pattern alterations below critical threshold values of space occupation by vegetation patches could lead to large changes in the hydrological connectivity of the landscape. When exceeding these degradation thresholds, the ecosystems become "leaky" or dysfunctional, meaning that the remaining vegetation pattern has, to a great extent, lost the ability to obstruct and capture the surface flow of water runoff and sediments [*Ludwig et al.*, 2007]. These reductions in the availability of resources might promote a self-reinforcing degradation trend that increases the persistence of the dysfunctional landscape state, even when the drivers of degradation have been eliminated [*Suding et al.*, 2004]. In fact, significant decreases in available water (i.e., soil moisture) and nutrients for plant growth could greatly reduce the amount and size of the vegetated patches and their associated sink capacity, further increasing hydrological connectivity in the landscape and the loss of resources [*Moreno-de las Heras et al.*, 2010].

[6] Landscape connectivity is currently perceived as a unifying concept for the analysis of land degradation and desertification processes, being intimately linked to the ecosystem functionality of water-limited environments [*Okin et al.*, 2009]. Although the existence of dryland degradation thresholds associated to the hydrological connectivity and functionality of these landscapes has been extensively explored using both conceptual and theoretical approaches [*Davenport et al.*, 1998; *Ludwig et al.*, 2005; *Turnbull et al.*, 2008; *King et al.*, 2011], their actual existence in real landscapes has been rarely documented [*Ludwig et al.*, 2002, 2007]. Furthermore, it is still unclear how different environmental drivers (e.g., different types of disturbances) can influence these degradation or ecosystem stability thresholds [*Peters et al.*, 2006; *Field et al.*, 2011]. Remote sensing of vegetation, now routinely available, is a useful tool that can facilitate the analysis of these relationships. In fact, high resolution remote sensing allows the study of fine-scale spatial processes in these patchy landscapes [*Scanlon et al.*, 2007]. In addition, satellite-derived vegetation indices, such as the Normalized Difference Vegetation Index (NDVI), supply important information on the structure (e.g., green biomass) and productivity of these systems, hence offering valuable cues for the assessment of ecosystem health and function [*Anderson et al.*, 1993; *Holm et al.*, 2003b; *Evans and Geerken*, 2004].

[7] The objective of this study is to explore the impact of landscape degradation on the hydrological connectivity and ecosystem functionality of patterned semiarid landscapes. We specifically expect to improve our understanding on (i) the existence of degradation thresholds on these dryland systems, and (ii) the dependency of the landscape degradation trends on the type of disturbance. Our study focuses on patchy (banded) shrublands displayed by Mulga in semiarid Australia. We implement a methodology based on the coupled analysis of remotely sensed vegetation patterns and elevation data to evaluate the hydrological connectivity in several Mulga landscapes subjected to different levels of disturbance. We also estimate the rainfall-use efficiency of these landscapes by analyzing the relationship between rainfall amount and the observed temporal trends of remotely sensed NDVI (as a proxy for vegetation response to rainfall). Finally, we use a simple model of vegetation thinning (i.e., reduction of fractional vegetation cover) to analyze the

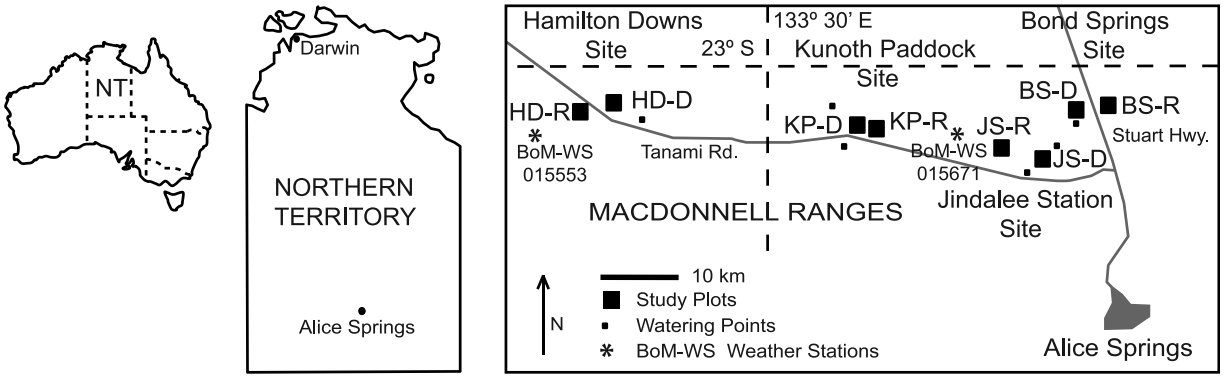

Figure 1. Location map.

response of the landscape hydrological connectivity to different types and degrees of disturbance.

2. Materials and Methods

2.1. Study Sites

[8] This work has been carried out in four study sites located in the Northern Territory (Australia), near Alice Springs: the Bond Springs, Jindalee Station, Kunoth Paddock and Hamilton Downs sites. These sites are situated in a 500 km^2 area with homogeneous climate, soil, landform and vegetation characteristics on the Burt Plain, a region of very gently sloping landforms north of the MacDonnell Ranges (Figure 1). Annual precipitation in the area is 300 mm, with a summer maximum, and annual potential evapotranspiration is 2200 mm [*Raupauch et al.*, 2001]. *Low* [1978] described vegetation patterns within these sites as (quasi) periodic, with groves of Mulga trees (*Acacia aneura*) and perennial grasses (e.g., *Eragrostis eriopoda*, *Monochather paradoxa*) creating strips and bands (typically of 10–30 m width) aligned to contours of the gently sloping terrain (0.3°–0.6° slope), which are separated by intergroves that are scarcely covered by ephemeral species (e.g., *Aristida contorta*). Soils are massive red earths, Haplargid [*Soil Survey Staff*, 2010], which in bare and barely covered conditions develop robust physical crusts that readily generate water runoff, while the same soil type under Mulga canopy has high infiltration potential [*Greene et al.*, 2001].

[9] These sites are representative of Australian grazing areas, and are extensively grazed by commercial livestock (mainly beef cattle) as well as local populations of red kangaroos. Disturbance caused by grazing can be locally intense, depending on livestock management and the distance to the watering points [*Pickup et al.*, 1994]. Other types of disturbances, such as wildfires, can also be important in the area. In each of the four study sites, two different areas (of 1.5 × 1.5 km^2) were selected: a disturbed plot, as well as a well-preserved plot used as reference. In order to limit human disturbance effects in the reference landscapes, these plots (BS-R, JS-R, KP-R and HD-R, Figures 2a–2d) were selected in nearly pristine areas located more than 3 km away from the watering points. Disturbed plots (BS-D, JS-D, KP-D and HD-D, Figures 2a–2d) were selected in areas close to major watering points and stocking routes. These disturbed plots span the most distinctive disturbed areas in the study 500 km^2 region. The major perturbation effects in the disturbed Bond Spring, Jindalee Station and Kunoth Paddock plots (BS-D, JS-D and KP-D) are due to cattle grazing. However, for the disturbed plot located in the Hamilton Downs site (HD-D), the major source of disturbance was a wildfire that occurred in September 2001 [*Berg and Dunkerley*, 2004].

2.2. Quantifying Hydrological Connectivity

[10] Hydrological connectivity measures for this study have been obtained using the coupled analysis of high resolution remotely sensed vegetation patterns and digital elevation models of the sites, and the flowlength calculator described below.

[11] Remotely sensed vegetation data was obtained from a set of four-band geo-referenced and pan-sharpened QuickBird scenes (0.6 m pixel resolution, 30 km^2 area each scene) captured on July 2006 (Bond Springs and Jindalee Station sites), August 2005 (Kunoth Paddock site) and September 2006 (Hamilton Downs site). We used the multispectral information of the scenes to generate binary maps of vegetation by applying a supervised classification technique with a global accuracy of 96% (SD 1%) [*Moreno-de las Heras et al.*, 2011a]. The procedure comprised: (i) the determination of the characteristic spectral signatures for both the vegetated Mulga groves and the barely covered intergroves in representative training areas within the scenes, and (ii) the categorization of every pixel in the scenes into one of the two aforementioned classes (i.e., vegetation and bare soil pixels) to create binary maps, using the maximum likelihood criteria. These binary maps were subsampled to obtain the two 1.5 × 1.5 km^2 plots for each study site described in the previous section and shown in Figures 2a–2d.

[12] Elevation information was derived from a 1-arc second (approximately 30 m) digital elevation model (DEM) originally produced by the NASA Shuttle Radar Topographic Mission (SRTM) and recently post-processed by the CSIRO Division of Land and Water and Geosciences Australia (1-Second SRTM-derived DEM-S, Version 1.0) [*Tickle et al.*, 2010]. The elevation data was resampled to match the 0.6 m grid-based vegetation maps obtained from the QuickBird scenes. We used harmonic splines for interpolation, since this technique has shown a good performance for resampling SRTM data at finer resolution [*Grohmann and Steiner*, 2008]. Resampled elevation data was pitfilled using the *Planchon and Darboux* [2002] algorithm. Less than 5% DEM-S pixels contained in the study sites were affected by pitfilling.

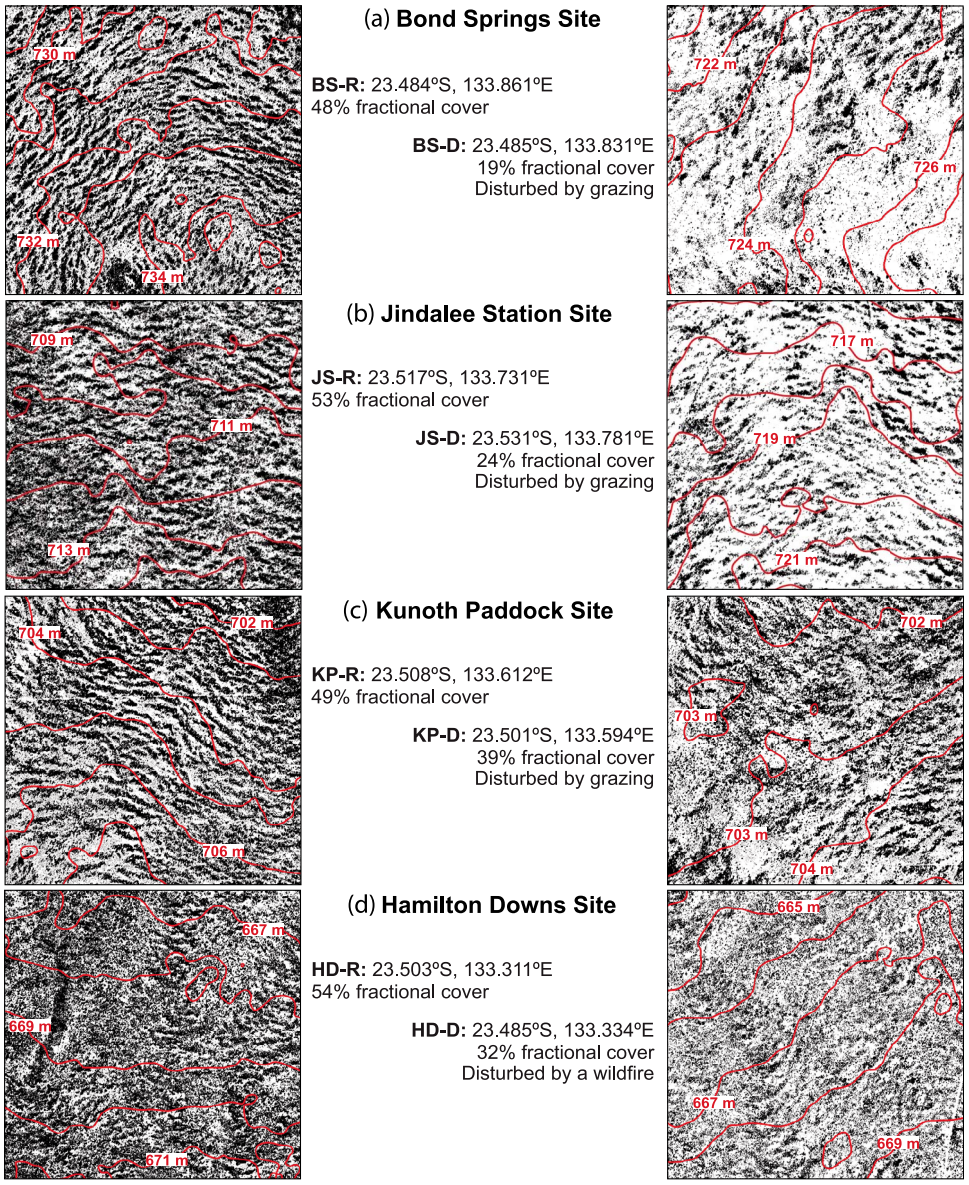

Figure 2. Study sites: vegetation pattern (derived from remotely sensed QuickBird scenes that were taken in 2005–2006), elevation contours (obtained from the SRTM-derived DEM-S) and general characteristics (center coordinates, fractional cover and major source of disturbance) of the studied *Acacia aneura* (Mulga) semiarid landscapes. Reference plots: BS-R, JS-R, KP-R, and HD-R. Disturbed plots: BS-D, JS-D, KP-D, HD-D. Plot size is 1.5×1.5 km^2.

[13] We used the flowlength calculator developed by *Mayor et al.* [2008] for the quantification of landscape hydrological connectivity. This calculator determines the potential length of the flowpath for each cell within the binary vegetation maps, using the DEM data and the D8 flow routing algorithm [*O'Callaghan and Mark*, 1984]. Vegetation pixels are identified as runoff sinks, while bare soil pixels are identified as runoff sources. The runoff path downslope of each cell is determined in the neighboring steepest descent direction, until a sink (i.e., a vegetation pixel) or boundary pixel is reached. The flowlength (FL) or total length of the flowpath originated in each cell is computed. For each plot, we estimated the cumulative probability distribution function (CDF) of flowlengths, defined as the probability of flowpaths being of equal or longer size than a determined flowlength (i.e., Probability Flowpath $\geq$ FL). Flowlength CDF differences between reference and disturbed conditions for each site were analyzed using two-sample Kolmogorov-Smirnov tests. In addition, the mean flowlength was calculated for each plot as an integrative indicator of the landscape hydrological connectivity.

2.3. Rainfall-Use Efficiency Estimations

[14] The NDVI is a remote sensed chlorophyll-sensitive vegetation index that, for semiarid landscapes, strongly correlates with green biomass levels (i.e., leaves and green stems of woody vegetation plus aboveground herbaceous biomass) [*Anderson et al.*, 1993; *du Plessis*, 1999; *Huete et al.*, 2002].

Uncertainties in relating NDVI to vegetation can be important in drylands, especially due to mixing effects associated with soil brightness and variations in soil background reflectance [*Huete*, 1988; *Okin et al.*, 2001]. Nonetheless, studies examining primary production and phenology of different vegetation types have demonstrated the usefulness of NDVI for the analysis of vegetation dynamics in arid and semiarid environments [*Holm et al.*, 2003b; *Popp et al.*, 2009; *Choler et al.*, 2010]. As explained in previous studies, the analysis of time series of NDVI and precipitation provides information on the capacity of dryland landscapes to convert rainfall into biomass [*Holm et al.*, 2003b; *Evans and Geerken*, 2004]. We have adopted this rationale to estimate rainfall-use efficiency in our study areas.

[15] We used NDVI data from the Moderate Resolution Imaging Spectroradiometer (MODIS), obtained from the NASA Warehouse Inventory Search Tool (https://wist.echo.nasa.gov/~wist/api/imswelcome/). We compiled a two-year series (from January 2005 to January 2007) of NDVI with a temporal resolution of 8 days, using the signals of the MODIS Terra and Aqua satellites (i.e., collection 5, MOD13Q1 and MYD13Q1 products, respectively). The pixel resolution is 232 m (after re-projection to UTM coordinates), so for each 1.5×1.5 km^2 study plot we calculated the mean NDVI signal of the landscape (averaged from 42 pixels). The temporal span of the series analyzed (2005–2007) was selected to evaluate the dynamic vegetation response (captured by the NDVI signal) to rainfall variability, over a period that corresponded to the vegetation pattern captured by the QuickBird scenes (obtained between August 2005 and September 2006). To reduce the interference of cloud anomalies in the compiled NDVI series, we checked the reliability summary layer of the acquired MODIS products and discarded those NDVI values that did not have the highest quality flag value (less than 2% of data). Finally, in order to reduce the inherent noise of the NDVI data series we have fitted a cubic smoothing spline polynomial to the data trends [*Furrer et al.*, 2011].

[16] Daily rainfall data for this analysis was obtained from local rain gauges provided by the Australian Bureau of Meteorology (http://www.bom.gov.au/climate/data/). Specifically, we used rainfall records from two weather stations located between 5 and 15 km away from the study plots (BoM-WS 015553 and 015671, Figure 1a).

[17] Primary production in drylands has been usually shown to display a slow response to precipitation [*du Plessis*, 1999; *Scanlon et al.*, 2002; *Evans and Geerken*, 2004]. In order to detect the impact of rainfall variability on plant production in our study sites, we studied the correlation between the NDVI and rainfall series using various rainfall accumulation periods and lag times between rainfall and plant response. The values of lag time and accumulation period that maximized those correlations were selected, and the corresponding slope of the linear regression (between NDVI and lagged/accumulated rainfall) was identified. We used the slope of this relationship as a surrogate for the rainfall-use efficiency (RUE) of the landscapes describing the rate of conversion of rainfall into NDVI (or green biomass). In order to test for differences in RUE between the reference and disturbed conditions within each site, we analyzed a series of four linear models (a model for each study site) predicting NDVI values as a function of the amount of rainfall, the presence of disturbances, and their interaction: NDVI $\sim$ Rainfall + Disturbance + Rainfall $\times$ Disturbance, where Rainfall is a continuous predictor (the selected lagged/accumulated rainfall series) and Disturbance is a factor (the presence/absence of grazing and wildfire signals in the landscapes). The interaction (i.e., Rainfall $\times$ Disturbance) indicates whether there is a significant effect of the analyzed disturbances in the slope of the NDVI-rainfall relationship, or in other words, a significant change in the RUE of the landscapes under disturbed conditions.

2.4. Simulation Analysis

[18] In order to assess the impact of different types of disturbances in the hydrological connectivity of these landscapes, we developed and used two different thinning algorithms for the simulation of vegetation removal (for example by death, fire or animal consumption). One of these algorithms was developed to randomly remove vegetation pixels from binary maps of vegetation. It simulates a non-selective (random) disturbance that homogeneously distributes the rate of plant mortality (or removal) throughout the landscape. The second algorithm selectively removes pixels of vegetation located at the edges of the vegetation patches. It simulates a selective disturbance that concentrates plant removal on those areas that are spatially most accessible (i.e., the external edges of the vegetation patches). Details on these two vegetation-removal algorithms are included in the auxiliary material of this paper.[1]

[19] We modeled vegetation thinning (by plant removal due to for example grazing or fire), by applying these algorithms to the more pristine areas of our landscapes. We therefore selected a homogeneous 750×750 m^2 section of vegetation pattern from one of our reference Mulga landscapes (BS-R) and we have applied the two different vegetation-removal algorithms. We used both algorithms to obtain a sequence of increasingly "degraded" plots by progressively reducing the fractional cover of the landscape to different "pattern degradation" levels (e.g., 40, 30 … 3, 1% fractional cover). Then, we applied the flowlength calculator [*Mayor et al.*, 2008] to obtain quantitative hydrological connectivity measures (i.e., flowlength CDF and mean flowlength of the landscape) for these modeled disturbance scenarios. These simulations must be interpreted as a simplified approach. In fact, this modeling methodology simulates an instantaneous alteration of the hydrologic behavior of each pixel in response to the removal or death of vegetation (i.e., the hydrologic behavior of the pixels change from sink to source of water runoff and sediments after vegetation removal). Consequently, these algorithms do not capture delayed and/or variable dynamics induced by changes in soil properties (e.g., in water infiltration capacity, soil structure, etc.) after vegetation thinning.

3. Results

3.1. Observed Pattern Changes and Degradation Effects

[20] Visual inspection and analysis of spatial organization of the vegetation pattern in the Bond Springs and Jindalee

[1] Auxiliary materials are available in the HTML. doi:10.1029/2011JG001839.

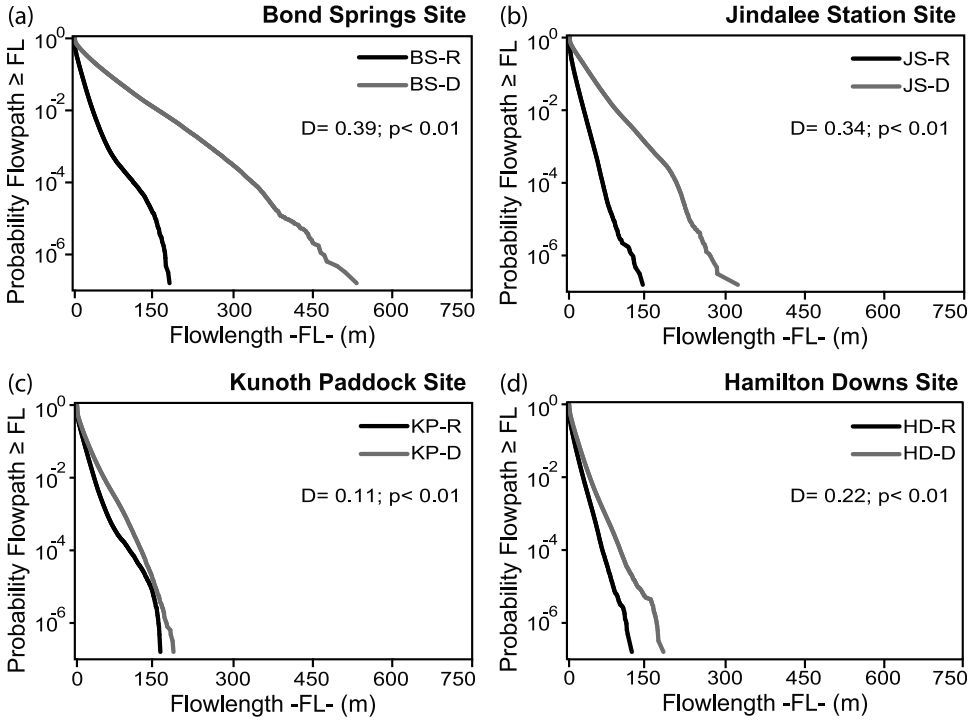

Figure 3. Cumulative probability distribution function (CDF) of flowlengths in the studied *Acacia aneura* (Mulga) semiarid landscapes. Two-sample Kolmogorov-Smirnov D statistics and p levels for testing differences between reference and disturbed plots are shown. Reference plots: BS-R, JS-R, KP-R, and HD-R. Disturbed plots: BS-D, JS-D, KP-D, HD-D.

Station plots affected by grazing (BS-D and JS-D, respectively) shows very important differences when compared to that of their reference plots (BS-R and JS-R, Figures 2a and 2b). Vegetation in BS-R and JS-R is spatially arranged in well-defined Mulga bands aligned along the terrain contours, covering about 50% of the space. Contrasting with these well-preserved conditions, Mulga patches in the disturbed BS-D and JS-D plots are largely fragmented (covering 19%–24% of space, respectively) and have lost, to a great extent, the characteristic banding. In the case of the Kunoth Paddock site (Figure 2c), pattern variations observed in the plot affected by grazing (KP-D) are less significant. In comparison with the well-preserved banded pattern of the reference plot (KP-R), the disturbed KP-D plot shows a more fragmented banded pattern, though bands are still visible. In addition, differences in global space occupation by Mulga patches (i.e., fractional cover) between these two plots (49% and 39% for the KP-R and KP-D plots, respectively) are less dramatic than those previously indicated for the Bond Springs and Jindalee Station plots. For the Hamilton Downs site (Figure 2d), alterations of vegetation cover caused by the wildfire in the HD-D plot are fairly important in comparison with the vegetation of the reference plot (HD-R). This impact is especially significant in terms of fractional cover for the disturbed plot (32% versus the 54% of the undisturbed plot). This loss is homogeneously distributed throughout the landscape and, as a result, the disturbed HD-D plot displays sparse vegetation groves (i.e., with less vegetation cover), but with a global appearance of the spatial vegetation pattern organization (i.e., shape of pattern) that is very similar to that observed in the reference HD-R plot.

3.2. Hydrological Connectivity of the Landscapes

[21] Figure 3 shows the cumulative probability distribution functions (CDF) of flowlengths for the studied sites, illustrating the impact of observed vegetation pattern alterations on the landscape hydrological connectivity. Two-sample Kolmogorov-Smirnov tests indicate significant differences at $p < 0.01$ between reference and disturbed plots for all the studied sites. However, graphical interpretation of the CDFs shows that for some sites these variations are not very pronounced. For the Bond Springs and Jinadalee Station sites (Figures 3a and 3b), the probability of finding long flowpaths (e.g., longer than 100–250 m) is considerable higher in the plots affected by grazing (BS-D and JS-D) than in the nearly pristine landscapes (BS-R and JS-R). Interestingly, the flowlength CDF is markedly wider for the disturbed BS-D plot, which has a maximum flowlength (560 m) three times larger than that of the reference BS-R plot (180 m). For the disturbed JS-D plot the CDF is also notably wider, reaching a maximum flowlength (305 m) about two times larger than that of the reference JS-R plot (140 m). Differences in the CDFs of the Kunoth Paddock and Hamilton Downs sites are less pronounced (Figures 3c and 3d). In fact, the flowlength CDFs of the Kunoth Paddock plots are very similar regardless of their conservation status (e.g., maximum flowlength is 160 and 180 m in KP-R and KP-D, respectively; Figure 3c). For the Hamilton Downs site (Figure 3d), the probability of finding long flowpaths in the plot affected by the wildfire (HD-D) is slightly higher than in the reference plot (HD-R). In this case, maximum flowlength in the disturbed (HD-D) and pristine (HD-R) plots are 190 m and 120 m, respectively.

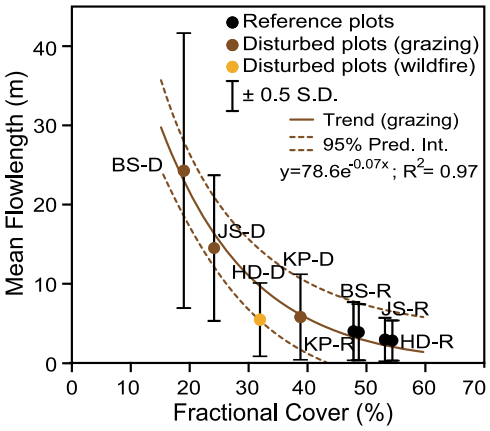

Figure 4. Variability of the landscape hydrological connectivity (plot-averaged flowlength) as a function of fractional cover (fraction of space covered by vegetation) for the studied *Acacia aneura* (Mulga) semiarid landscapes. Fitted exponential function is significant at $p < 0.01$. Reference plots: BS-R, JS-R, KP-R, and HD-R. Disturbed plots: BS-D, JS-D, KP-D, HD-D.

[22] Figure 4 presents the variability of the landscape hydrological connectivity (i.e., mean flowlength) as a function of fractional cover (i.e., fraction of space covered by vegetation) for all study plots in these landscapes. Connectivity variations between the four reference plots (HD-R, JS-R, KP-R and BS-R, with fractional cover between 54% and 48%) are very small (from 3 to 4 m). The landscape hydrological connectivity of the disturbed plots in the Kunoth Paddock and Hamilton Downs sites (KP-D and HD-D, 39%–32% fractional cover) is moderately higher (about 6 m). Connectivity variations between these five plots are minor compared to the hydrological connectivity of the disturbed Jindalee Station and Bond Spring plots (JS-D and BS-D). In fact, the JS-D landscape (24% fractional cover) shows a mean flowlength of 14 m, while for the disturbed BS-D plot (19% fractional cover) the mean flowlength is 24 m.

[23] Overall, the relationship between the landscape hydrological connectivity of the plots and their fractional cover is strongly nonlinear. The trend obtained from data corresponding to both the reference landscapes (HD-R, JS-R, KP-R and BS-R) and the disturbed plots affected by grazing (KP-D, JS-D and BS-D) can be closely approximated by an exponential function (Figure 4). The wildfire-disturbed Hamilton Downs plot (HD-D) deviates from this general (grazing) trend, as indicated by its relative position to the 95% prediction interval (Figure 4). In fact, HD-D shows a mean flowlength (6 m at 32% fractional cover) that is significantly lower than that predicted by the fitted exponential (grazing) curve (approx. 9 m).

3.3. Rainfall-Use Efficiency of the Landscapes

[24] Maximum correlations between the NDVI and precipitation time series for the four sites (eight plots) were obtained for rainfall lag times between 0 and 10 days, and periods of rainfall accumulation between 175 and 260 days (black dots in Figures 5a–5d). In order to facilitate the comparison of the NDVI-rainfall relationships, we selected for the analysis an optimal value defined by the maximum of the surface obtained as the sum of the correlations between the NDVI and the lagged accumulation rainfall series for all locations (i.e., sum of the eight surfaces shown in Figures 5a–5d). This global maximum correlation value was obtained for a lag time of 5 days and a rainfall accumulation period of 219 days. Figures 6a–6d present the NDVI-rainfall relationships obtained using these values of lag time and rainfall accumulation period for the eight plots. In the case of the Bond Spring and Jindalee Station sites (Figures 6a and 6b), the slope of the NDVI-rainfall relationship for the disturbed BS-D and JS-D plots (1.6×10^{-4} mm^{-1}) is considerably smaller than that for the reference BS-R and JS-R plots (2.2×10^{-4} mm^{-1}). This means that for these two sites, the rainfall-use efficiency (i.e., conversion of rainwater into NDVI) for the plots affected by grazing (BS-D and JS-D) is notably lower than that of the pristine landscapes (BS-R and JS-R). The interaction between the amount of rainfall and the presence of disturbances for the prediction of the NDVI values in these two sites confirms that the observed reductions in rainfall-use efficiency are statistically significant (Rainfall × Disturbance: $F_{1,182} = 9.98$, $p < 0.01$ for the Bond Springs site, and $F_{1,182} = 6.42$, $p = 0.01$ for the Jindalee Station site). Conversely, for the Kunoth Paddock site (Figure 6c), this effect is not significant (Rainfall × Disturbance: $F_{1,182} = 0.37$, $p = 0.54$). In fact, the slope of the NDVI-rainfall relationship in the Kunoth Paddock plot affected by grazing (KP-D: 2.2×10^{-4} mm^{-1}) is approximately the same as that of the reference plot (KP-R: 2.3×10^{-4} mm^{-1}). Finally, for the Hamilton Downs site (Figure 6d) the slope of the relationship in the plot affected by the wildfire (HD-D: 2.5×10^{-4} mm^{-1}) is slightly higher than that of the reference plot (HD-R: 2.2×10^{-4} mm^{-1}), although this change is not statistically significant (Rainfall × Disturbance, $F_{1,182} = 0.66$, $p = 0.42$).

[25] Figures 7a and 7b show the variability of rainfall-use efficiency (i.e., slope in the NDVI-rainfall relationship) for the different plots analyzed as a function of their fractional cover, and landscape hydrological connectivity. Differences in rainfall-use efficiency between the four reference plots (HD-R, JS-R, KP-R and BS-R) and the disturbed plots of the Kunoth Paddock and Hamilton Downs sites (KP-D and HD-D) are small. In fact, the NDVI-rainfall slope for all these plots (with 54%–32% fractional cover and 3–6 m mean flowlength) varies slightly between 2.2×10^{-4} and 2.5×10^{-4} mm^{-1}. However, the rate of conversion of rainfall into vegetation greenness (or growth) obtained from the NDVI-rainfall relationship in the disturbed plots of the Jindalee Station and Bond Spring sites (JS-D and BS-D: 1.6×10^{-4} mm^{-1}, with 24%–19% fractional cover and 14–24 m mean flowength) is about 30% lower than those of the other sites.

[26] As seen in Figure 7, changes in rainfall-use efficiency caused by grazing in the analyzed landscapes (i.e., the general trend excluding the HD-D plot that was affected by a wildfire) are characterized by an abrupt nonlinear reduction as a function of landscape conditions (expressed as either a reduction in fractional cover or an increase in landscape hydrological connectivity). Fitted step functions indicate that this abrupt change occurs at approximately 32% fractional cover (Figure 7a) and 10 m mean flowlength (Figure 7b). The widldfire-disturbed HD-D plot significantly deviates from this general behavior found for the grazing sites, showing

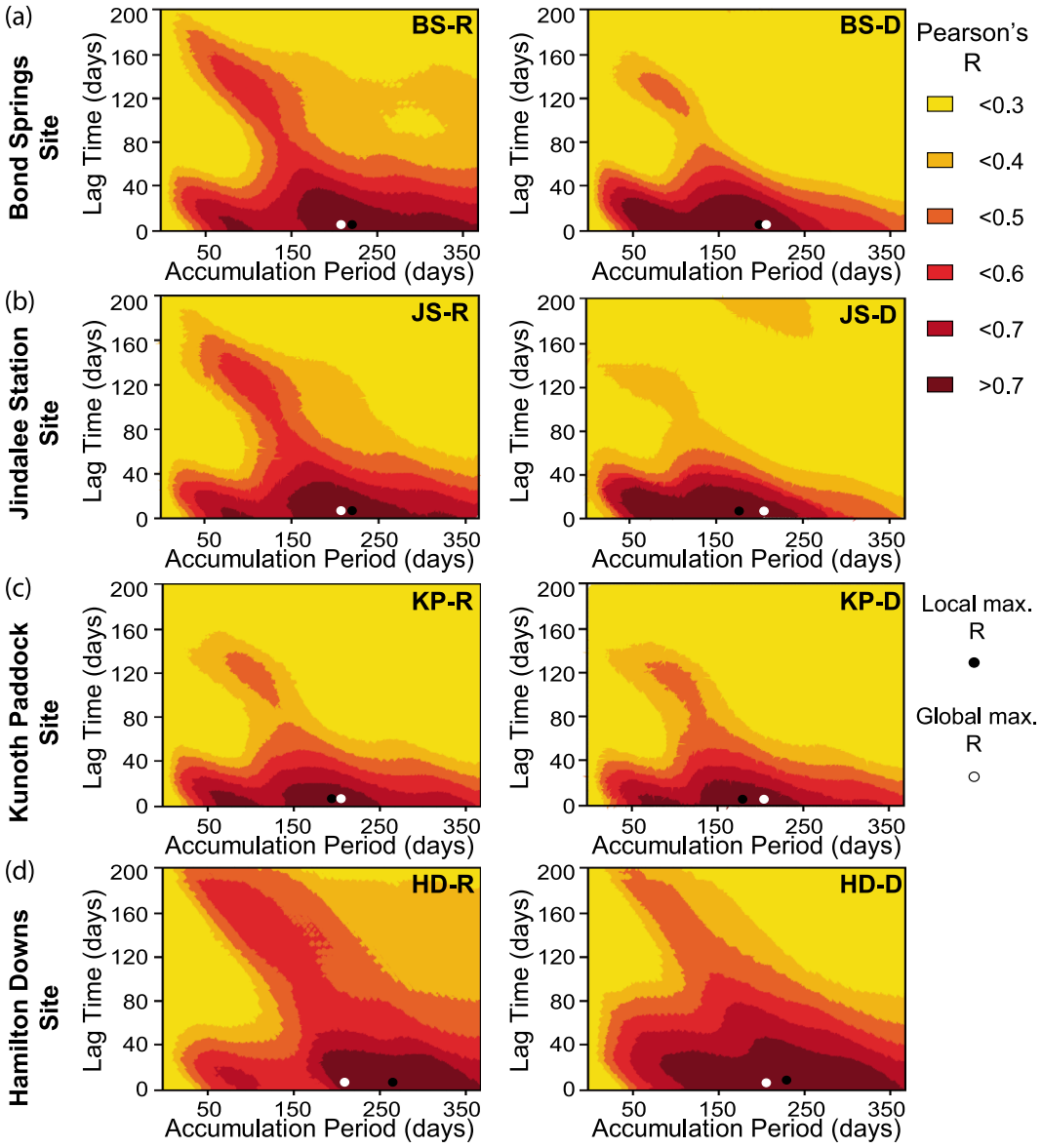

Figure 5. Correlation (Pearson's R) between the NDVI and precipitation in the studied *Acacia aneura* (Mulga) semiarid landscapes using different precipitation lag times and rainfall accumulation periods. Local maximum correlation (Local max. R) for each site, as well as the values of lag time and accumulated period used for analysis (5 and 219 days, respectively; Global max. R) are shown. Reference plots: BS-R, JS-R, KP-R, and HD-R. Disturbed plots: BS-D, JS-D, KP-D, HD-D.

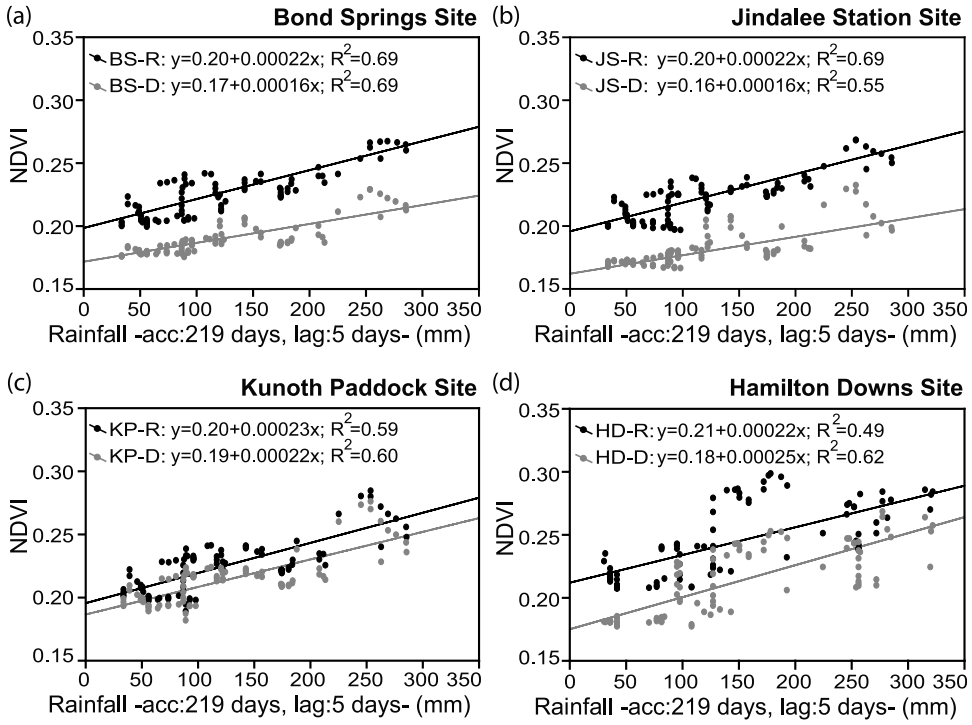

Figure 6. Relationship between the NDVI and rainfall in the studied *Acacia aneura* (Mulga) semiarid landscapes using a precipitation lag time and rainfall accumulation period of 5 and 219 days, respectively. Reported functions are significant at $p < 0.01$. Reference plots: BS-R, JS-R, KP-R, and HD-R. Disturbed plots: BS-D, JS-D, KP-D, HD-D.

rainfall-use efficiency values slightly higher than those of the other plots with higher fractional cover and lower landscape hydrological connectivity.

3.4. Simulated Degradation Trends

[27] Differences in the evolution of vegetation pattern modeled using the non-selective and selective vegetation-removal algorithms are obvious from visual inspection of the simulated degradation trends presented in Figures 8a and 8b. The shape of the original vegetation pattern is better preserved along the disturbance gradient obtained using the non-selective algorithm that randomly removes pixels of vegetation from the landscape (Figure 8a). In this case, vegetation pixels are evenly removed from the entire vegetation clusters. Consequently, the remaining vegetation pixels are still clustered into vegetation patches that conserve their

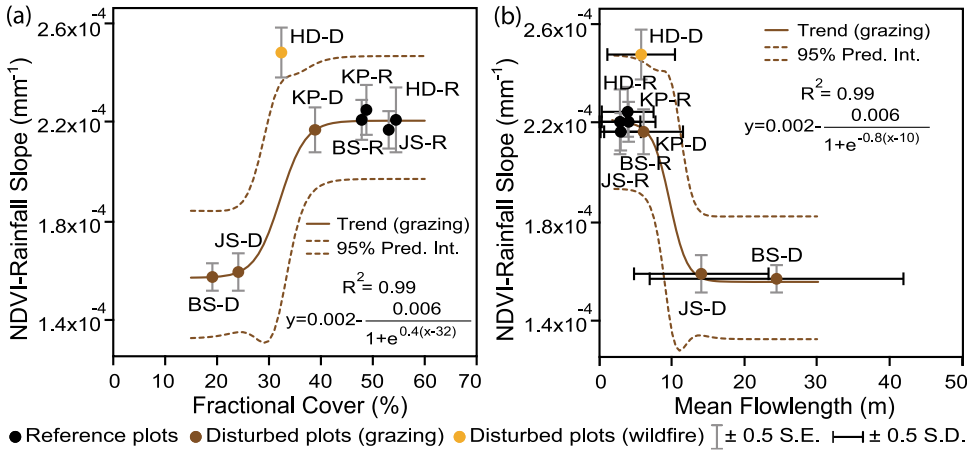

Figure 7. Variability of rainfall-use efficiency (slope of the NDVI-rainfall relationship) as a function of (a) fractional cover (fraction of space covered by vegetation) and (b) landscape hydrological connectivity (mean flowlength) for the studied *Acacia aneura* (Mulga) semiarid landscapes. Fitted step functions are significant at $p < 0.01$. Reference plots: BS-R, JS-R, KP-R, and HD-R. Disturbed plots: BS-D, JS-D, KP-D, HD-D.

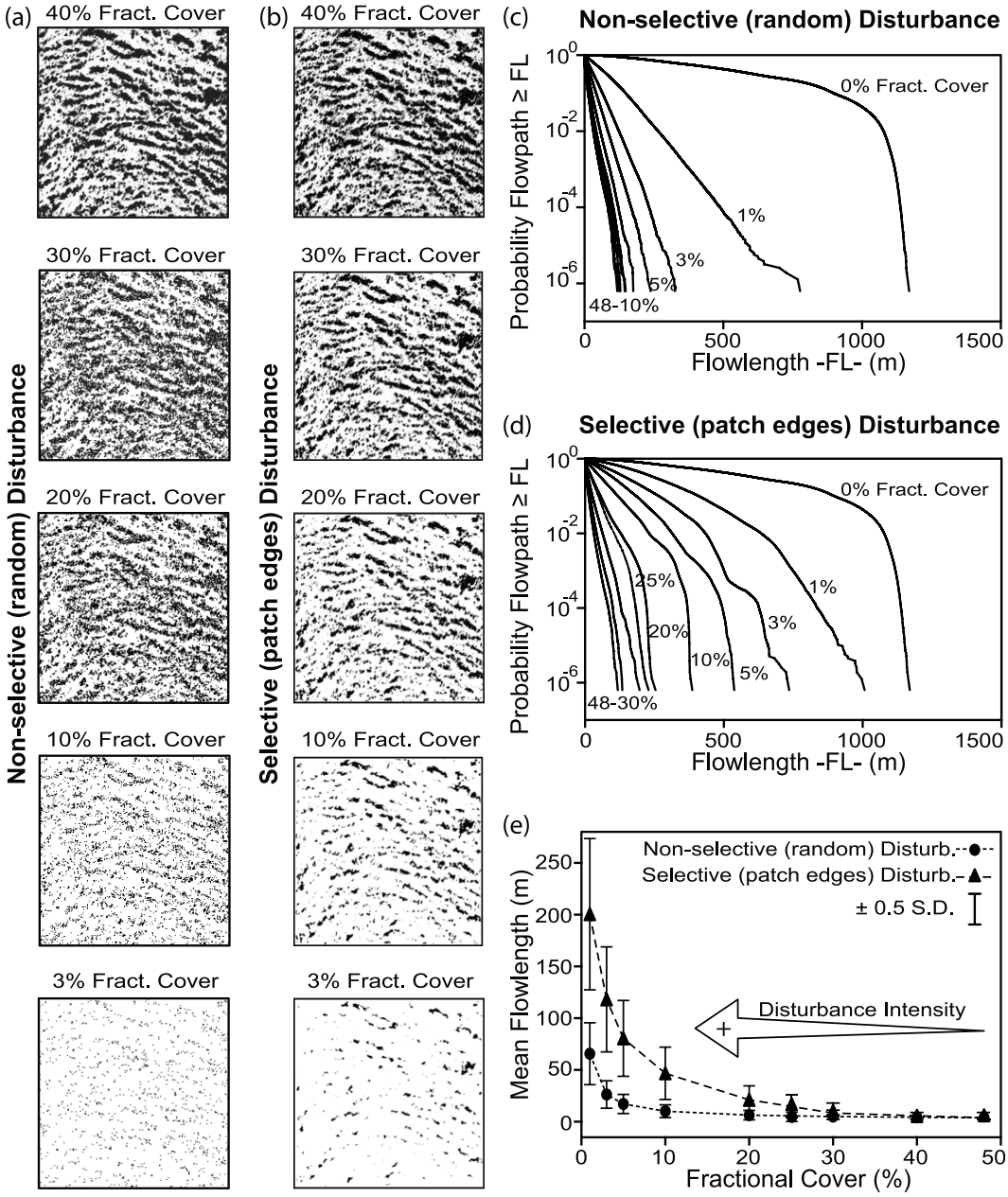

Figure 8. Simulated degradation trends: (a–b) effects of the simulated non-selective (random) and selective (patch edges) disturbances in the spatial organization of vegetation, (c–d) cumulative probability distribution function (CDF) of flowlengths for different degradation levels modeled using the simulated (non-selective and selective) disturbances, (e) variability of the landscape hydrological connectivity (plot averaged flowlength) as a function of fractional cover (fraction of space covered by vegetation) for different degradation levels modeled using the simulated (non-selective and selective) disturbances. Initial vegetation pattern for the simulations has been obtained from a homogeneous 750 × 750 m^2 fraction of the reference BS-R landscape.

original shape, even at the higher disturbance levels with lower fractional cover (e.g., 10%). For the other algorithm, which selectively removes vegetated pixels from the edges of the patches, it can be observed that along the degradation trend (Figure 8b) the clusters decrease in size but vegetation cover within each patch remains approximately constant. Consequently, at landscape fractional cover values between 20% and 30%, the general shape of the original vegetation pattern is lost. Overall, under severely degraded pattern conditions, the simulated non-selective disturbance generates a noisy landscape (i.e., remaining vegetation is widely dispersed throughout the landscape), while the simulated selective disturbance generates a barren landscape with some scattered vegetation spots.

[28] The cumulative probability distribution functions (CDF) of flowlengths reveal important differences on the hydrological connectivity of these two simulated degradation processes. For the simulated non-selective disturbance

(Figure 8c), changes in the flowlength CDF are very small for vegetation fractional covers above 5–10%. On the other hand, changes in the flowlength CDF for the landscapes simulated using the selective disturbance algorithm (Figure 8d) reflect a dramatic increase in the probability of finding longer flowpaths when the fractional cover drops below 20–30%. These changes in hydrological connectivity along the simulated degradation trends display a strong nonlinear behavior (Figure 8e). In other words, small reductions in the fractional cover of the landscape below certain breakpoint levels, lead to very large increases in the mean flowlength of the site. For the non-selective disturbance, mean flowlength reaches values close to 10 m at 10% fractional cover. A small change below this fractional cover produces a rapid and large nonlinear increase in the landscape hydrological connectivity. For the selective disturbance, this large nonlinear increase is reached when the fractional cover of the site is reduced below the 30%, for which the mean flowlength is about 11 m.

4. Discussion

4.1. Hydrological Connectivity and Rainfall-Use Efficiency of the Landscapes

[29] Our results, derived from remote sensing of banded Mulga vegetation, highlight the importance of the spatial organization of vegetation for the connectivity of runoff source areas (i.e., bare or barely covered areas), and its relevance for ecosystem functionality. The spatial arrangement of vegetation largely controls the redistribution of water, sediments and nutrients throughout the landscape [*Franz et al.*, 2012]. Therefore, important repercussions could be expected from the alteration of vegetation patterns [*Puigdefabregas et al.*, 1999; *Wilcox et al.*, 2003; *Okin et al.*, 2009]. Here, the comparison between the reference and disturbed plots reveals that alterations in the amount and spatial distribution of vegetation cover have a direct impact on the landscape hydrological connectivity, with an increase in the probability of finding longer flowpaths for the degraded sites (Figure 3). This effect is especially significant in the disturbed BS-D and JS-D plots (Figures 3a and 3b), where the high abundance of long flowpaths (e.g., those with flowlength longer than 100–250 m) increases the likelihood of having larger runoff losses and erosion through these landscapes. As previously discussed in the literature, such an increase in the connectivity of the runoff source areas (i.e., bare patches) has not only consequences for the hydrological response of the landscapes but also for their ecosystem functionality [*Wu et al.*, 2000; *Ludwig et al.*, 2005; *Popp et al.*, 2009]. In fact, we find that for the disturbed BS-D and JS-D plots, the NDVI-rainfall relationships suggest a reduction of about 30% in the conversion rate of rainfall into vegetation greenness (or green biomass), indicating a large decrease in the rainfall-use efficiency of these landscapes (Figures 6a and 6b). This decrease is in good agreement with reductions in landscape rainfall-use efficiency recorded in other severely disturbed patchy dryland ecosystems. For example, *Holm et al.* [2003a] reported reductions of about 20% in rainfall-use efficiency for degraded patchy Chenopod shrublands in Western Australia, and an exhaustive review of drylands around the world by *Le Houerou* [1984] indicated reductions of up to 65% in the rainfall-use efficiency for severely disturbed landscapes. In addition, modeling results in banded Mulga shrublands suggested that alterations in the spatial organization of vegetation could produce up to 40% reduction in the primary productivity of these landscapes [*Ludwig et al.*, 1999].

[30] A tightly coupled association between the hydrological connectivity (i.e., mean flowlength) and ecosystem functionality (i.e., rainfall-use efficiency) of the landscapes is suggested by our results (Figure 7b). These results clearly distinguish two contrasting (alternative) ecosystem states: (i) a group of functional landscapes (the reference BS-R, JS-R, KP-R and HD-R, as well as the disturbed KP-D and HD-D plots) with low hydrological connectivity (plot averaged flowlength: 3–6 m) and high rainfall-use efficiency (Rainfall-NDVI conversion rate: $2.2–2.5 \times 10^{-4}$ mm^{-1}), and (ii) two leaky or dysfunctional landscapes (the disturbed BS-D and JS-D plots) with high hydrological connectivity (24 m and 14 m, respectively) and low rainfall-use efficiency (1.6×10^{-4} mm^{-1}). Previous empirical research by *Mayor et al.* [2008] found that landscape-level hydrological connectivity, expressed as average flowlength (i.e., the mean of all flowpath lengths within the landscape), largely explains the delivery of water runoff and sediments in patchy dryland landscapes at large scales. Therefore, the high hydrological connectivity of the BS-D and JS-D landscapes provides an explanation for the low rainfall-use efficiency of these disturbed ecosystems: a significant fraction of the rainwater flows out the system (as runoff), and it is consequently not available for the production of green biomass. In other words, the high continuity of surface water flow between fine and larger scales (i.e., from patch to hillslope or landscape) results in the low ecosystem ability to redistribute and capture water runoff for plant growth [*Ludwig et al.*, 2002; *Turnbull et al.*, 2008; *Okin et al.*, 2009; *Dunkerley*, 2010].

[31] Our empirical observations of patchy Mulga shrublands subjected to different disturbance levels support the idea that landscape degradation processes in drylands may take place in an abrupt, rather than gradual manner [*Noy-Meir*, 1975; *Walker et al.*, 1981; *Scheffer et al.*, 2001; *Rietkerk et al.*, 2004; *D'Odorico et al.*, 2007; *King et al.*, 2011]. In fact, detailed exploration of the relationships between the integrity of the analyzed ecosystems (expressed either as the fractional cover of Mulga vegetation or their hydrological connectivity) and rainfall-use efficiency (Figures 7a and 7b) clearly suggest an abrupt landscape degradation response. The study plots with fractional cover above 32% and mean flowlength below 10 m display functional conditions (i.e., a high rainfall-use efficiency), while the dysfunctional BS-D and JS-D plots (19%–24% fractional cover, 24–14 m mean flowlength) appear to have passed a landscape degradation threshold. This observation is in agreement with previous results by *Davenport et al.* [1998] who, using percolation theory, suggested that the functionality of patchy semiarid ecosystems is prone to sharp changes in the ecosystem's ability to redistribute and capture surface flows of water and sediments. They based their hypothesis on observations of the hydrological response of two patchy semiarid landscapes located in New Mexico. In spite of having very similar features (e.g., soils, topography, type of vegetation), these two landscapes largely differed on the broad-scale water runoff and erosion rates, that were found to be mainly associated to small differences in vegetation patterns (i.e., fractional cover). A similar behavior has been

suggested for banded semiarid landscapes in southwest Niger, where the presence of critical levels of "landscape permeability" to overland flow has been associated to the rapid degradation of these patterned ecosystems [*Wu et al.*, 2000].

4.2. Influence of Disturbance Type

[32] The simulated degradation trends confirm the nonlinear behavior of the changes observed in our banded Mulga study landscapes (Figure 8). In fact, we found that small alterations in the vegetation cover below particular breakpoint values trigger large increases in the landscape hydrological connectivity. However, these breakpoint values are strongly dependent on the type of disturbance, with values about 20–30% for the simulated selective (patch-edges) disturbance, and around 10% fractional cover for the non-selective (random) disturbance (Figure 8e). The degradation trend modeled using the algorithm that selectively removes vegetated pixels from the edges of the vegetated patches closely captures some key characteristics of the observed vegetation changes caused by grazing in the disturbed BS-D, JS-D and KP-D plots. For example, the mean flowlengths for the modeled disturbance situations (21 m, 15 m and 6 m at 20%, 25% and 40% fractional cover) closely match the values recorded in the real landscapes (24 m, 14 m and 6 m at 19%, 24% and 39% fractional cover, respectively for BS-D, JS-D and KP-D). This is not surprising, since the impact of grazing/browsing from both livestock and wild animals is usually concentrated in the most accessible areas of the vegetation patches (i.e., their edges). These results indicate that grazing may lead to a substantial increase in the hydrological connectivity of banded Mulga landscapes when the fractional cover drops below 20–30%, thus intensely affecting the ecosystem's primary production through the loss of water resources. This observation is in agreement with previous observations reported in the literature [*Noble et al.*, 1998; *Holm et al.*, 2003a; *Popp et al.*, 2009] of dramatic long-term disturbance effects for heavily grazed patchy semiarid landscapes.

[33] The hydrological connectivity changes caused by wildfire in the disturbed Hamilton Downs landscape (HD-D) are better captured by the simulations from the non-selective (random) algorithm, which homogeneously distributes plant removal (or mortality) throughout the landscape. The mean flowlength in the burned HD-D plot (6 m for 32% fractional cover) deviates from the empirical (grazing) trend illustrated in Figure 4, and is closer to that obtained from the simulated random disturbance (5 m for 30% fractional cover) than to that obtained from the simulated selective disturbance (11 m for 30% fractional cover). In addition, the visual appearance of the pattern alterations modeled using the simulated random disturbance (i.e., clusters of remaining vegetated pixels that globally preserve the original shape of the vegetation patches, Figure 8a) closely resemble the spatial changes observed in HD-D (Figure 2d). However, the limited extent of our analysis for wildfire-affected areas does not allow us to draw broader conclusions on the general correspondence between the effects of fire in the studied landscapes and the disturbance simulated by the non-selective (random) process. Previous studies carried out in Mulga shrublands affected by wildfires have indicated that *A. aneura* is very sensitive to fire, with plants frequently though not invariably killed if the whole canopy is burnt [*Griffin and Friedel*, 1984; *Hodkinson*, 2002]. The resprouting capacity of Mulga is rather low (usually only 10–30% burned trees resprout after fire), so regeneration occurs primarily from seeds [*Wright and Clarke*, 2007]. Preserving the dead trees within the affected Mulga groves has important repercussions for the maintenance of the hydrological functionality in these disturbed landscapes [*Berg and Dunkerley*, 2004]. They offer some protection to the ground surface from wind and sun, and still have capacity to intercept rainfall, reducing raindrop impact and generating steamflow that enhances the recharge of soil moisture. Likewise, fallen dead Mulga trees play a significant role, developing log mounds with enhanced biological activity that obstruct the flow of water runoff and sediments [*Tongway and Ludwig*, 1989]. Provided that dead trees are not extensively removed (e.g., for firewood harvesting) and the affected area has not been previously (or afterwards) disturbed by heavy grazing or other recent wildfires, patchy Mulga shrublands show a high capacity to regenerate vegetation after fire and maintain the landscape hydrological functionality [*Hodkinson*, 2002; *Murphy et al.*, 2010].

[34] Previous studies have suggested that low disturbance levels (e.g., light grazing pressure) could enhance the spatial redistribution of water runoff within the landscape and thus, increase the productivity of patchy ecosystems [*Noble et al.*, 1998; *Urgeghe et al.*, 2010]. They explained this effect considering that there might exist an optimal level of fractional cover (lower than those of the pristine landscapes) for which runoff is re-concentrated in the vegetation patches, stimulating plant production. Our results suggest that such positive effect (though very weak) could have taken place in the area affected by the wildfire of the Hamilton Downs site. As reflected by the slope of the rainfall-NDVI relationships (Figure 6d), the rainfall-use efficiency in the burned HD-D plot (2.5×10^{-4} mm^{-1}, 32% fractional cover) is slightly higher (although not statistically different) than that recorded in the reference HD-R plot (2.2×10^{-4} mm^{-1}, 54% fractional cover). More research is required to disentangle these complex responses. We hypothesize that such a positive effect is more likely for disturbances whose impact is homogeneously distributed throughout the landscape (which is the case for our non-selective disturbance simulations), since they produce a more effective reduction in the global biomass of the system without drastically increasing the interconnection of bare soil areas.

[35] We want to emphasize that our empirical results and our simple simulations give important but limited insight into the complex effects induced by disturbances in these systems. Disturbances can also show important variations on the extent and/or intensity of their impact on the different landscape components (e.g., vegetation and soil) [*Peters et al.*, 2006; *Field et al.*, 2011]. Understanding these variable impacts and their associated response time scales is of key importance for the analysis of catastrophic ecosystem transitions in patterned landscapes, particularly since it is well known that landscape resilience (i.e., the ecosystem ability to recover pre-disturbance conditions) in these systems is largely dependent on the long-term established vegetation-soil positive feedbacks [*Tongway and Ludwig*, 1996, 2001; *Dunkerley*, 2010]. In fact, for the same amount of alterations in vegetation (i.e., same reduction in fractional cover and

same spatial disturbance), a more significant impact can be anticipated for different types of disturbances. For example, long-term grazing and wildfires can cause large alterations in soil properties (e.g., soil compaction and surface crusting, depletion of soil organic matter, fire-induced soil hydrophobicity), while other disturbances do not have immediate repercussions on soil quality (e.g., wood harvesting activities).

4.3. Concluding Remarks and Management Implications

[36] Our analysis indicates a strong nonlinear behavior of degradation processes in patchy (banded) Mulga shrublands of semiarid Australia. This result agrees with the ecosystem-stability principles discussed, during the last decades, in both theoretical and empirical studies focusing on the origin, functioning and maintenance of patterned dryland ecosystems [*Noy-Meir*, 1973, 1975; *Schlesinger et al.*, 1990; *Tongway and Ludwig*, 2001; *Wilcox et al.*, 2003; *D'Odorico et al.*, 2007]. This dynamic behavior implies that small changes in landscape conditions can trigger a large shift in ecosystem function if a critical degradation threshold is exceeded. Our findings indicate that these degradation thresholds in semiarid Mulga are related to large nonlinear increases in the connectivity of bare and barely covered areas (i.e., runoff generating areas). This shift affects landscape function, producing a sharp reduction in the rainfall-use efficiency of vegetation. In fact by exceeding this landscape degradation threshold, the ecosystems become "leaky" or dysfunctional, since an important amount of water runoff (and other limiting resources, such as soil and nutrients) is routed out of the landscape, becoming unavailable for plant production [*Ludwig et al.*, 2005; *Turnbull et al.*, 2008; *Okin et al.*, 2009].

[37] Rangeland management strategies must account for the close relationship between the spatial organization of vegetation and ecosystem function in drylands, and include measures to preserve the hydrological functionality of these landscapes. From a practical point of view, our results suggest that the amount of alterations in the vegetation pattern that landscapes can absorb, while still remaining hydrologically functional, is higher in the case of disturbances that are homogeneously distributed throughout the landscape. These observations imply that, in order to minimize the impact of wood harvesting activities (i.e., firewood and timber collection) in patchy Mulga vegetation, the concentration of the impact on the edges of the patches must be avoided, as well as the complete elimination of vegetation patches on particular landscape locations, which is what usually occurs during harvesting operations due to accessibility [*Driscoll et al.*, 2000]. Instead, homogeneous wood collection throughout the landscape and within the vegetation patches should be encouraged to avoid the generation of long connected flowpaths that could increase the permeability of the landscape to overland flow. In addition, wood-harvesting activities must be excluded from patchy Mulga shrublands affected by wildfires to preserve the hydrological functionality of these disturbed landscapes [*Berg and Dunkerley*, 2004].

[38] In banded as well as other types of patterned ecosystems (e.g., striped, labyrinthine), maintenance of patchiness integrity (i.e., the spatial organization of vegetation) is an important general principle that land managers must acknowledge [*Tongway and Ludwig*, 2001; *Turnbull et al.*, 2008; *Dunkerley*, 2010; *King et al.*, 2011]. Water-vegetation feedbacks can notably increase the stability of dysfunctional or degraded ecosystem states, as a result hindering the restoration of the ecosystem functions [*Valentin et al.*, 1999; *Wu et al.*, 2000; *Wilcox et al.*, 2003; *Suding et al.*, 2004]. In these situations, only methodologies directed to restore a desirable landscape hydrological connectivity by breaking up the long connected pathways of runoff can help to recover the ecosystem functionality. Indeed, experimental work by *Tongway and Ludwig* [1996, 2011] concluded that vegetation patches can be restored by building spatial structures that trap and store water runoff and sediments (e.g., brush piles parallel to land contours).

[39] There is global concern that these ecosystem changes, under particular circumstances, can be largely irreversible [*Noy-Meir*, 1975; *Scheffer et al.*, 2001; *Rietkerk et al.*, 2004]. Carbon isotope research in Mulga landscapes [*Bowman et al.*, 2007] indicated that these patterned ecosystems have remained relatively stable over the past 1000 years, implying that Mulga bands are considerably resilient to variable weather conditions and natural disturbances. Irreversible ecosystem transitions in semiarid Mulga are more likely to occur in landscapes with extensively developed drainage networks (i.e., rills and gullies), which strongly facilitate the routing of water runoff [*Wakelin-King*, 1999]. Rill and gully erosion processes not only provide permanent drainage pathways for runoff losses throughout the landscape, but also largely disrupt the long-term plant-soil positive feedbacks that confer high resilience to these patchy landscapes [*Puigdefabregas et al.*, 1999; *Wilcox et al.*, 2003; *Moreno-de las Heras et al.*, 2011b]. In fact, modeling results [*Saco and Rodriguez*, 2012] have suggested that the long-term stability and recovery capacity of patchy landscapes are severely constrained in high-erosion risk areas (i.e., high slope and/or soil erodibility landscapes), which in Mulga shrublands is confirmed by a general scarcity of vegetation bands in areas with slope gradient higher than 2° [*Murphy et al.*, 2010]. Long-term changes in the mean and/or variability of climatic factors can also influence the reversibility of these ecosystem transitions. In fact, changes in precipitation patterns in drylands (and specifically the increase in the recurrence of severe droughts) are currently perceived as chronic contributing factors to the irreversible degradation of disturbed semiarid and arid ecosystems [*van Auken*, 2000; *Suding et al.*, 2004; *Clifford et al.*, 2011].

[40] Overall our results highlight the usefulness of indicators derived from landscape hydrological connectivity analysis for monitoring landscape health in semiarid and arid ecosystems. These indicators could help to prevent the development and/or consolidation of barren ecosystem states in dryland landscapes, which would otherwise require very expensive human interventions for functionality restoration. Future work could benefit from recent advances in geophysical sensors for quantifying plant available water [*Robinson et al.*, 2008; *Zreda et al.*, 2008]. This will help to increase the understanding of the complex processes involved in the use of water by dryland vegetation (e.g., surface redistribution of water, root uptake, transpiration, etc.) and the impact of landscape degradation in these processes.

[41] **Acknowledgments.** This work was supported by the project DP0774184 funded by the Australian Research Council. M. Moreno-de las

Heras is supported by a postdoctoral fellowship funded by the University of Alcalá. We wish to thank Angeles G. Mayor for providing us with the flow-length calculator and Carlos Riveros and Luis Cayuela for technical advice. The 1-Second SRTM-derived DEM-S was provided under a collaboration research agreement with the NSW Office of Environment and Heritage. The manuscript benefited from the helpful comments of two anonymous referees.

References

Anderson, G. L., J. D. Hanson, and R. H. Haas (1993), Evaluating Landsat Thematic Mapper derived vegetation indices for estimating above-ground biomass on semiarid rangelands, *Remote Sens. Environ.*, *45*, 165–175, doi:10.1016/0034-4257(93)90040-5.

Berg, S. S., and D. L. Dunkerley (2004), Patterned Mulga near Alice Springs, central Australia, and the potential threat of firewood collection on this vegetation community, *J. Arid Environ.*, *59*, 313–350, doi:10.1016/j.jaridenv.2003.12.007.

Bowman, D. M. J. S., G. S. Boggs, L. D. Prior, and E. S. Krull (2007), Dynamics of Acacia aneura-Triodia boundaries using carbon (^{14}C and $\delta^{13}C$) and nitrogen ($\delta^{15}N$) in soil organic matter in central Australia, *Holocene*, *17*, 311–318, doi:10.1177/0959683607076442.

Choler, P., W. Sea, P. Briggs, M. Raupauch, and R. Leuning (2010), A simple ecohydrological model captures essentials of seasonal leaf dynamics in semiarid tropical grasslands, *Biogeosciences*, *7*, 907–920, doi:10.5194/bg-7-907-2010.

Clifford, M. J., N. S. Cobb, and M. Buenemann (2011), Long-term tree cover dynamics in a Pinyon-Juniper woodland: Climate-change-type resets successional clock, *Ecosystems (N. Y.)*, *14*, 949–962, doi:10.1007/s10021-011-9458-2.

Davenport, D. W., D. D. Breshears, B. P. Wilcox, and C. D. Allen (1998), Viewpoint: Sustainability of piñon-juniper ecosystems—A unifying perspective of soil erosion thresholds, *J. Range Manage.*, *51*, 231–240, doi:10.2307/4003212.

Deblauwe, V., N. Barbier, P. Couteron, O. Lejeune, and J. Bogart (2008), The global biogeography of semi-arid periodic vegetation patterns, *Global Ecol. Biogeogr.*, *17*, 715–723, doi:10.1111/j.1466-8238.2008.00413.x.

D'Odorico, P., K. Caylor, G. S. Okin, and T. M. Scanlon (2007), On soil moisture-vegetation feedbacks and their possible effects on the dynamics of dryland ecosystems, *J. Geophys. Res.*, *112*, G04010, doi:10.1029/2006JG000379.

Driscoll, D., M. Milkovits, and D. Freudenberger (2000), *Impact and Use of Firewood in Australia*, Environ. Australia, Canberra, Australia.

Dunkerley, D. L. (2010), Ecogeomorphology in the Australian drylands and the role of biota in mediating the effects of climate change on landscape processes and evolution, in *Australian Landscapes, Geol. Soc. Spec. Publ. 346*, edited by P. Bishop and B. Pillans, pp. 87–120, Geol. Soc. of London, London, U. K.

Dunkerley, D. L., and K. L. Brown (1999), Banded vegetation near Broken Hill, Australia: Significance of surface roughness and soil physical properties, *Catena*, *37*, 75–88, doi:10.1016/S0341-8162(98)00056-3.

du Plessis, W. P. (1999), Linear regression relationships between NDVI, vegetation and rainfall in Etosha National Park, Namibia, *J. Arid Environ.*, *42*, 235–260, doi:10.1006/jare.1999.0505.

Evans, J., and R. Geerken (2004), Discrimination between climate and human-induced dryland degradation, *J. Arid Environ.*, *57*, 535–554, doi:10.1016/S0140-1963(03)00121-6.

Field, J. P., D. D. Breshears, J. J. Whicker, and C. B. Zou (2011), Interactive effects of grazing and burning on wind- and water-driven sediment fluxes: Rangeland management implications, *Ecol. Appl.*, *21*, 22–32, doi:10.1890/09-2369.1.

Franz, T. E., K. K. Caylor, E. G. King, J. M. Nordbotten, M. A. Celia, and I. Rodriguez-Iturbe (2012), An ecohydrological approach to predicting hillslope-scale vegetation patterns in dryland ecosystems, *Water Resour. Res.*, *48*, W01515, doi:10.1029/2011WR010524.

Furrer, R., D. Nychka, and S. Sain (2011), Smoothing spline regression (sreg), in *fields: Tools for Spatial Data, R Package Version 6.5.2*, pp. 143–147, Inst. for Stat. and Math., Vienna. [Available at http://cran.r-project.org.]

Greene, R. S. B., C. Valentin, and M. Esteves (2001), Runoff and erosion processes, in *Banded Vegetation Patterning in Arid and Semiarid Environments, Ecological Processes and Consequences for Management*, *Ecol. Stud.*, 149, edited by D. J. Tongway, C. Valentin, and J. Seghieri, pp. 52–76, Springer, New York.

Griffin, G. F., and M. H. Friedel (1984), Effects of fire on central Australian rangelands. II: Changes in tree and shrub populations, *Aust. J. Ecol.*, *9*, 395–403, doi:10.1111/j.1442-9993.1984.tb01376.x.

Grohmann, C. H., and S. S. Steiner (2008), SRTM resample with short distance-low nugget kriging, *Int. J. Geogr. Inf. Sci.*, *22*, 895–906, doi:10.1080/13658810701730152.

Hodkinson, K. C. (2002), Fire regimes in acacia wooded landscapes: Effects on functional processes and biological diversity, in *Flammable Australia: The Fire Regimes and Biodiversity of a Continent*, edited by R. A. Bradstock, J. E. Williams, and A. M. Gill, pp. 259–277, Cambridge Univ. Press, Cambridge, UK.

Holm, A. M., S. W. Cridland, and M. L. Roderick (2003a), The use of time-integrated NOAA NDVI data and rainfall to assess landscape degradation in the arid shrubland of Western Australia, *Remote Sens. Environ.*, *85*, 145–158, doi:10.1016/S0034-4257(02)00199-2.

Holm, A. M., I. W. Watson, W. A. Loneragan, and M. A. Adams (2003b), Loss of patch-scale heterogeneity on primary productivity and rainfall-use efficiency in Western Australia, *Basic Appl. Ecol.*, *4*, 569–578, doi:10.1078/1439-1791-00187.

Huete, A. R. (1988), A soil-adjusted vegetation index (SAVI), *Remote Sens. Environ.*, *25*, 295–309, doi:10.1016/0034-4257(88)90106-X.

Huete, A., K. Didan, T. Miura, E. P. Rodriguez, X. Gao, and L. G. Ferreira (2002), Overview of the radiometric and biophysical performance of the MODIS vegetation indices, *Remote Sens. Environ.*, *83*, 195–213, doi:10.1016/S0034-4257(02)00096-2.

King, E. G., T. E. Franz, and K. K. Caylor (2011), Ecohydrological interactions in a degraded two-phase mosaic dryland: Implications for regime shifts, resilience and restoration, *Ecohydrology*, doi:10.1002/eco.260, in press.

Klausmeier, C. A. (1999), Regular and irregular patterns in semiarid vegetation, *Science*, *284*, 1826–1828, doi:10.1126/science.284.5421.1826.

Le Houerou, H. N. (1984), Rain use efficiency: A unifying concept in arid-land ecology, *J. Arid Environ.*, *7*, 213–247.

Low, W. A. (1978), The physical and biological features of Kunoth Paddock in central Australia, *Tech. Pap. 4*, CSIRO Div. Land Resour. Manage., Melbourne, Australia.

Ludwig, J. A., D. J. Tongway, and S. G. Mardsen (1999), Stripes, strands or stipples: Modelling the influence of three landscape banding patterns on resource capture and productivity in semi-arid woodlands, Australia, *Catena*, *37*, 257–273, doi:10.1016/S0341-8162(98)00067-8.

Ludwig, J. A., R. W. Eager, G. N. Bastin, V. H. Chewings, and A. C. Liedloff (2002), A leakiness index for assessing landscape function using remote sensing, *Landscape Ecol.*, *17*, 157–171, doi:10.1023/A:1016579010499.

Ludwig, J. A., B. P. Wilcox, D. D. Breshears, D. J. Tongway, and A. I. Imeson (2005), Vegetation patches and runoff-erosion as interacting ecohydrological processes in semiarid landscapes, *Ecology*, *86*, 288–297, doi:10.1890/03-0569.

Ludwig, J. A., G. N. Bastin, V. H. Chewings, R. W. Eager, and A. C. Liedloff (2007), Leakiness: A new index for monitoring the health of arid and semiarid landscapes using remotely sensed vegetation cover and elevation data, *Ecol. Indic.*, *7*, 442–454, doi:10.1016/j.ecolind.2006.05.001.

Macfadyen, W. A. (1950), Soil and vegetation in British Somaliland, *Nature*, *165*, 121, doi:10.1038/165121a0.

May, R. H. (1977), Thresholds and breakpoints in ecosystems with a multiplicity of stable states, *Nature*, *269*, 471–477, doi:10.1038/269471a0.

Mayor, A. G., S. Bautista, E. E. Small, M. Dixon, and J. Bellot (2008), Measurement of the connectivity of runoff source areas as determined by vegetation pattern and topography: A tool for assessing potential water and soil losses in drylands, *Water Resour. Res.*, *44*, W10423, doi:10.1029/2007WR006367.

McDonald, A. K., R. J. Kinucan, and L. E. Loomis (2009), Ecohydrological interactions within banded vegetation in the northeastern Chihuahuan Desert, USA, *Ecohydrology*, *2*, 66–71, doi:10.1002/eco.40.

Moreno-de las Heras, M., J. M. Nicolau, L. Merino-Martin, and B. P. Wilcox (2010), Plot-scale effects on runoff and erosion along a slope degradation gradient, *Water Resour. Res.*, *46*, W04503, doi:10.1029/2009WR007875.

Moreno-de las Heras, M., P. M. Saco, G. R. Willgoose, and D. J. Tongway (2011a), Assessing landscape structure and pattern fragmentation in semiarid ecosystems using patch-size distributions, *Ecol. Appl.*, *21*, 2793–2805, doi:10.1890/10-2113.1.

Moreno-de las Heras, M., R. Diaz-Sierra, J. M. Nicolau, and M. A. Zavala (2011b), Evaluating restoration of man-made slopes: A threshold approach balancing vegetation and rill erosion, *Earth Surf. Processes Landforms*, *36*, 1367–1377, doi:10.1002/esp.2160.

Mueller, E. N., J. Wainwright, and A. J. Parsons (2008), Spatial variability of soil and nutrient characteristics of semi-arid grasslands and shrublands, Jornada basin, New Mexico, *Ecohydrology*, *1*, 3–12.

Murphy, B. P., P. Paron, L. D. Prior, G. S. Boggs, D. C. Franklin, and D. M. J. S. Bowman (2010), Using generalized autoregressive error models to understand fire-vegetation-soil feedbacks in mulga-spinifex landscape

mosaic, *J. Biogeogr.*, *37*, 2169–2182, doi:10.1111/j.1365-2699.2010.02359.x.

Noble, J. C., R. S. B. Greene, and W. J. Muller (1998), Herbage production following rainfall redistribution in a semi-arid Mulga (*Acacia aneura*) woodland in western New south Wales, *Rangeland J.*, *20*, 206–225, doi:10.1071/RJ9980206.

Noy-Meir, I. (1973), Desert ecosystems: Environment and producers, *Annu. Rev. Ecol. Syst.*, *4*, 25–51, doi:10.1146/annurev.es.04.110173.000325.

Noy-Meir, I. (1975), Stability of grazing systems: An application of predator-prey graphs, *J. Ecol.*, *63*, 459–481, doi:10.2307/2258730.

O'Callaghan, J. F., and D. M. Mark (1984), The extraction of drainage networks from digital elevation data, *Comput. Vis. Graph. Image Process.*, *28*, 323–344, doi:10.1016/S0734-189X(84)80011-0.

Okin, G. S., D. A. Roberts, B. Murray, and W. J. Okin (2001), Practical limits on hyperspectral vegetation discrimination in arid and semiarid environments, *Remote Sens. Environ.*, *77*, 212–225, doi:10.1016/S0034-4257(01)00207-3.

Okin, G. S., A. J. Parsons, J. Wainwright, J. E. Herrick, B. T. Bestelmeyer, D. C. Peters, and E. L. Fredrickson (2009), Do changes in connectivity explain desertification? *BioScience*, *59*, 237–244, doi:10.1525/bio.2009.59.3.8.

Peters, D. P. C., B. T. Bestelmeyer, J. E. Herrick, E. L. Fredickson, H. C. Monger, and K. M. Havstad (2006), Disentangling complex landscapes: New insights into arid and semiarid system dynamics, *BioScience*, *56*, 491–501, doi:10.1641/0006-3568(2006)56[491:DCLNII]2.0.CO;2.

Pickup, G., G. N. Bastin, and V. H. Chewings (1994), Remote-sensing-based condition assessment for nonequilibrium rangelands under large-scale commercial grazing, *Ecol. Appl.*, *4*, 497–517, doi:10.2307/1941952.

Planchon, O., and F. Darboux (2002), A fast, simple and versatile algorithm to fill the depressions of digital elevation models, *Catena*, *46*, 159–176, doi:10.1016/S0341-8162(01)00164-3.

Popp, A., M. Vogel, and F. Jeltsch (2009), Scaling up ecohydrological processes: Role of surface water flow in water-limited landscapes, *J. Geophys. Res.*, *114*, G04013, doi:10.1029/2008JG000910.

Puigdefabregas, J., A. Sole, L. Gutierrez, G. del Barrio, and M. Boer (1999), Scales and processes of water and sediment redistribution in drylands: Results from the Rambla Honda field site in SE Spain, *Earth Sci. Rev.*, *48*, 39–70, doi:10.1016/S0012-8252(99)00046-X.

Raupauch, M. R., J. M. Kirkby, D. J. Barret, and P. R. Briggs (2001), Balances of water, carbon, nitrogen and phosphorous in Australian landscapes: (I) Project description and results, *Tech. Rep. 40/01*, 40 pp., CSIRO Land and Water, Canberra, ACT.

Reynolds, J. F., et al. (2007), Global desertification: Building a science for dryland development, *Science*, *316*, 847–851, doi:10.1126/science.1131634.

Rietkerk, M., S. C. Dekker, P. C. de Ruiter, and J. van de Koppel (2004), Self-organized patchiness and catastrophic shifts in ecosystems, *Science*, *305*, 1926–1929, doi:10.1126/science.1101867.

Robinson, D. A., C. S. Campbell, J. W. Hopmans, B. K. Hornbuckle, S. B. Jones, R. Knight, F. Ogden, J. Selker, and O. Wendroth (2008), Soil moisture measurement for ecological and hydrological watershed-scale observatories: A review, *Vadose Zone J.*, *7*, 358–389, doi:10.2136/vzj2007.0143.

Rodriguez-Iturbe, I. (2000), Ecohydrology: A hydrologic perspective of climate-soil-vegetation dynamics, *Water Resour. Res.*, *36*, 3–9, doi:10.1029/1999WR900210.

Saco, P. M., and J. F. Rodriguez (2012), Modeling ecogeomorphic systems, in *Treatise on Geomorphology 2: Quantitative Modeling in Geomorphology*, edited by J. Shroder, Jr. and A. C. W. Baas, Academic, San Diego, Calif., in press.

Saco, P. M., G. R. Willgoose, and G. R. Hancock (2007), Eco-geomorphology of banded vegetation patterns in arid and semi-arid regions, *Hydrol. Earth Syst. Sci.*, *11*, 1717–1730, doi:10.5194/hess-11-1717-2007.

Scanlon, T. M., J. D. Albertson, K. K. Caylor, and C. A. Williams (2002), Determining land surface fraction cover from NDVI and rainfall time series for a savanna ecosystem, *Remote Sens. Environ.*, *82*, 376–388, doi:10.1016/S0034-4257(02)00054-8.

Scanlon, T. M., K. K. Caylor, S. A. Levin, and I. Rodriguez-Iturbe (2007), Positive feedbacks promote power-law clustering of Kalahari vegetation, *Nature*, *449*, 209–212, doi:10.1038/nature06060.

Scheffer, M., S. Carpenter, J. A. Foley, C. Folke, and B. Walker (2001), Catastrophic shifts in ecosystems, *Nature*, *413*, 591–596, doi:10.1038/35098000.

Schlesinger, W. H., J. F. Reynolds, G. L. Cunningham, L. F. Huenneke, W. M. Jarrell, R. A. Virginia, and W. G. Whitford (1990), Biological feedbacks in global desertification, *Science*, *247*, 1043–1048, doi:10.1126/science.247.4946.1043.

Soil Survey Staff (2010), *Keys to Soil Taxonomy*, 11th ed., U.S. Dep. of Agric. Nat. Resour. Conserv. Serv., Washington, D. C.

Suding, K. N., K. L. Gross, and G. R. Houseman (2004), Alternative states and positive feedbacks in restoration ecology, *Trends Ecol. Evol.*, *19*, 46–53, doi:10.1016/j.tree.2003.10.005.

Tickle, P., N. Wilson, C. Inskeep, J. Gallant, T. Dowling, and A. Read (2010), *1-Second SRTM-Derived Digital Elevation Models User Guide, Version 1.0.3*, 84 pp., Geosci. Australia/CSIRO Land and Water, Canberra, ACT.

Tongway, D. J., and J. A. Ludwig (1989), Mulga log mounds: Fertile patches in the semi-arid woodlands of eastern Australia, *Aust. J. Ecol.*, *14*, 263–268, doi:10.1111/j.1442-9993.1989.tb01436.x.

Tongway, D. J., and J. A. Ludwig (1996), Rehabilitation of semiarid landscapes in Australia: I. Restoring productive soil patches, *Restor. Ecol.*, *4*, 388–397, doi:10.1111/j.1526-100X.1996.tb00191.x.

Tongway, D. J., and J. A. Ludwig (2001), Theories on the origins, maintenance, dynamics and functioning of banded landscapes, in *Banded Vegetation Patterning in Arid and Semiarid Environments, Ecological Processes and Consequences for Management*, *Ecol. Stud.*, 149, edited by D. J. Tongway, C. Valentin, and J. Seghieri, pp. 20–31, Springer, New York.

Tongway, D. J., and J. A. Ludwig (2011), *Restoring Disturbed Landscapes: Putting Principles into Practice*, Island Press, New York, USA, doi:10.5822/978-1-61091-007-1.

Turnbull, L., J. Wainwright, and R. E. Brazier (2008), A conceptual framework for understanding semi-arid land degradation: Ecohydrological interactions across multiple-space and time scales, *Ecohydrology*, *1*, 23–34, doi:10.1002/eco.4.

Urgeghe, A. M., D. D. Breshears, S. N. Martens, and P. C. Beeson (2010), Redistribution of runoff among vegetation patch types: On ecohydrological optimality of herbaceous capture of run-on, *Rangeland Ecol. Manage.*, *63*, 497–504, doi:10.2111/REM-D-09-00185.1.

Valentin, C., J. M. d'Herbes, and J. Poesen (1999), Soil and water components of banded vegetation patterns, *Catena*, *37*, 1–24, doi:10.1016/S0341-8162(99)00053-3.

van Auken, O. W. (2000), Shrub invasions of North American semiarid grasslands, *Annu. Rev. Ecol. Syst.*, *12*, 352–356.

Wainwright, J., A. J. Parsons, W. H. Schlesinger, and A. D. Abrahams (2002), Hydrology-vegetation interactions in areas of discontinuous flow on a semi-arid bajada, southern New Mexico, *J. Arid Environ.*, *51*, 319–338, doi:10.1006/jare.2002.0970.

Wakelin-King, G. A. (1999), Banded mosaic ('tiger bush') and sheetflow plains: A regional mapping approach, *Aust. J. Earth Sci.*, *46*, 53–60, doi:10.1046/j.1440-0952.1999.00685.x.

Walker, B. H., D. Ludwig, C. S. Holling, and R. M. Peterman (1981), Stability of semiarid savanna grazing systems, *J. Ecol.*, *69*, 473–498, doi:10.2307/2259679.

Wilcox, B. P., D. D. Breshears, and C. D. Allen (2003), Ecohydrology of a resource-conserving semiarid woodland: Effects of scale and disturbance, *Ecol. Monogr.*, *73*, 223–239, doi:10.1890/0012-9615(2003)073[0223:EOARSW]2.0.CO;2.

Wright, B. R., and P. J. Clarke (2007), Resprouting responses of Acacia shrubs in the Western Desert of Australia–fire severity, interval and season influence interval, *Int. J. Wildland Fire*, *16*, 317–323, doi:10.1071/WF06094.

Wu, X. B., T. L. Thurow, and S. G. Whisenant (2000), Fragmentation and changes in hydrologic function of tiger bush landscapes, south-west Niger, *J. Ecol.*, *88*, 790–800, doi:10.1046/j.1365-2745.2000.00491.x.

Zreda, M., D. Desilets, T. P. A. Ferre, and R. L. Scott (2008), Measuring soil moisture content non-invasively at intermediate spatial scale using cosmic ray neutrons, *Geophys. Res. Lett.*, *35*, L21402, doi:10.1029/2008GL035655.